Curvelet-based palm vein biometric recognition

Qiang Li (李 强), Yan'an Zeng (曾延安)*, Xiaojun Peng (彭晓钧), and Kuntao Yang (杨坤涛)

College of Optoelectronic Science and Engineering, Huazhong University of Science and Technology, Wuhan 430074, China

**E-mail: zya401@126.com*

Received December 27, 2009

A novel personal recognition system utilizing palm vein patterns and a novel technique to analyze these vein patterns is presented. The technique utilizes the curvelet transform to extract features from vein patterns to facilitate recognition. This technique provides optimally sparse representations of objects along the edges. Principal component analysis (PCA) is applied on curvelet-decomposed images for dimensionality reduction. A simple distance-based classifier, such as the nearest-neighbor (NN) classifier, is employed. The experiments are performed using our palm vein database. Experimental results show that the algorithm reaches a recognition accuracy of 99.6% on the database of 500 distinct subjects.

OCIS codes: 100.5010, 100.3005, 100.7410.

doi: 10.3788/COL20100806.0577.

Personal recognition has become an important and in-demand technique for security access systems in the last decade. Biometric recognition techniques, such as face, iris, fingerprint, and palm print, have been intensively studied and developed to resolve security problems inherent in traditional personal recognition methods as well as to improve the reliability of these methods[1,2]. The main advantage of biometric recognition techniques over other conventional recognition methods, such as keys, passwords, and personal identification numbers (PINs), is that they are not prone to theft and loss, and do not rely on the memory of their users. Recently, hand vein pattern biometrics has attracted increasing interest from both research communities[3−5] and industries[6]. The uniqueness, stability, and strong immunity to forgery of vein patterns comprise a potentially good biometric that offers secure and reliable features for person identity recognition[7].

A research team from the Australian Institute of Security and Applied Technology[3] and a Korean research team both used active infrared (IR) imaging[4] techniques to acquire vein patterns at the back of the hand. Im *et al.* employed a charge-coupled device (CCD) camera to capture vein-pattern images[8]. Fujitsu Laboratories investigated the vein patterns in the palm side of the hand[6]. Lin *et al.* used the feature points of the vein patterns in the thermal images as a hand vein feature[5]. Wang *et al.* utilized minutiae features extracted from the vein patterns for recognition[7], and employed multiresolution wavelet analysis to extract the features in the hand vein images[9].

To our knowledge, no organization has carried out research on palm vein pattern biometric recognition technology except for Fujitsu; however, the company has not disclosed the features they used in any published research articles. In this letter, we propose a new personal recognition system using vein patterns in the palm side of the hand. This system is convenient for acquiring vein images compared with those based on vein patterns at the back of the hand. Since the palm vein patterns are curvilinear, we use curvelet transform to extract the features of palm vein patterns, because it has strong directional capability to represent edges and other singularities along curves. This method of extracting features has been reported since the introduction of second-generation curvelet transform in 2006[10]. Furthermore, the nearest-neighbor (NN) classifier is used to test the algorithm using our palm vein image database.

Biologically, a medical spectral window extends approximately from about 700 to 900 nm, in which light penetrates deeply into tissues, allowing for noninvasive investigation[11]. In addition, the hemoglobin in venous blood absorbs more IR radiation than the surrounding tissue[3]. Therefore, shooting an IR light beam at the desired body part could capture an image using a CCD camera with an attached IR filter. In the resulting image, the vein patterns appear darker than the surrounding parts and become easily discernible.

Since there is no palm vein pattern database which is publicly available for research, we thus designed our own near-IR palm vein image acquisition system to utilize palm vein patterns for recognition. In this system, we used an array of light-emitting diodes (LEDs) that emit IR light at a wavelength of 850 nm to shine IR light onto the palm side of the hand. On the same side, an IR CCD camera with spectral response peaking at a wavelength of around 850 nm was used to obtain the image of the palm vein. To dissipate the effect of visible light, an IR filter was mounted in front of the camera lens.

With this system, we constructed our own palm vein image database. It has 50 distinct participants and contains 1000 palm vein images from 100 different hands. The ages of these participants range from 18 to 60 years old. The images are in 256 level gray-scale of 640×480 pixels, and are stored in BMP format. Figure 1 shows several images from our database.

To increase recognition accuracy and reliability, the features of vein patterns were extracted from the same region in different palm vein images. We selected the second and fourth finger webs to fix the region known as region of interest region of interest (ROI). Figure 2(a) shows the result of the extracted ROI for the palm vein image in Fig. 1(a).

A 5×5 median filter was adopted to remove the speckling noise in the ROI image. The normalization process was performed to eliminate the influence of different

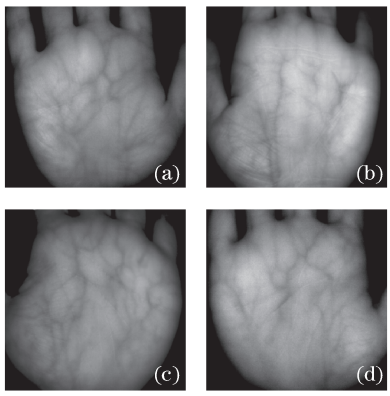

Fig. 1. Palm vein images of four different hands from our database.

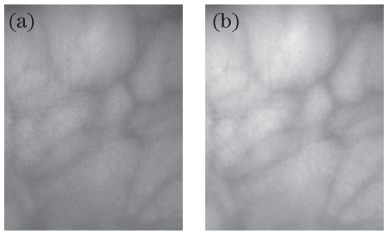

Fig. 2. ROI of original image and the result of image enhancement. (a) ROI for the palm vein image; (b) after noise reduction and normalization.

illumination intensity and time. The normalization methods employed in this work are similar to those suggested by Hong *et al.*[12].

Figure 2 shows the ROI of the original image and that enhanced with noise reduction and normalization.

Conceptually, the curvelet transform is a multiscale pyramid with many directions and positions at each length scale, as well as needle-shaped elements at fine scales[13]. Curvelet transform directly takes the edge as the basic representation element; it also provides optimally sparse representations of objects along the edges. Such representations are sparser than the wavelet decomposition of the object[14]. This was first developed by Candès *et al.* in 1999, while the second generation was introduced in 2006[10]. The latter is simpler, faster, and less redundant compared with the first-generation curvelet transform[15].

The curvelet transform and digital implementation are introduced as follows[10,13–17]. The digital curvelet takes Cartesian arrays of the form $f[t_1,t_2]$, $0 \le t_1$, $t_2<n$ as inputs, and outputs a collection of coefficients $c^D(j,\ell,k)$ expressed as

$$c^D(j,\ell,k) = \sum f[t_1,t_2]\overline{\phi^D_{j,\ell,k}[t_1,t_2]}, \tag{1}$$

where each $\phi^D_{j,\ell,k}$ is a digital curvelet waveform. In the digital definition, the window U_j does not exactly extract frequencies near the dyadic corona $\left\{2^j \le r \le 2^{j+1}\right\}$ and near the angle $\left\{-\pi \cdot 2^{-j/2} \le r \le \pi \cdot 2^{-j/2}\right\}$, and must be adapted to Cartesian arrays as illustrated in Fig. 3. The "Cartesian window" $\tilde{U}_j(\omega)$ is the product of the radial and angular window such as

$$\tilde{U}_j(\omega) = \tilde{W}_j(\omega)V_j(\omega), \tag{2}$$

where $\tilde{W}_j(\omega)$ and $V_j(\omega)$ obey certain admissibility conditions. Therefore, given a Cartesian array $f[t_1,t_2]$, $0 \le t_1$, $t_2<n$, we let $\hat{f}[t_1,t_2]$ denote its two-dimensional (2D) discrete Fourier transform as

$$\hat{f}[n_1,n_2] = \sum_{t_1,t_2}^{n-1} f[t_1,t_2]\mathrm{e}^{-\mathrm{i}2\pi(n_1t_1+n_2t_2)/n},$$
$$-n/2 \le n_1,n_2 < n/2. \tag{3}$$

Then the parabolic window $\tilde{U}_j[n_1,n_2]$ is supported on a rectangle P_j with length $L_{1,j}$ and width $L_{2,j}$,

$$P_j = \{(n_1,n_2) : n_{1,0} \le n_1 < n_{1,0} + L_{1,j},$$
$$n_{2,0} \le n_2 < n_{2,0} + L_{2,j}\}, \tag{4}$$

where $(n_{1,0}, n_{2,0})$ is the index of the pixel at the bottom-left of the rectangle.

Therefore, the fast discrete curvelet transform (FDCT) via unequally spaced fast Fourier transform (USFFT) is evaluated as

$$c^D(j,\ell,k) = \sum_{n_1,n_2\in P_j} \hat{f}[n_1,n_2-n_1\tan\theta_1]U_j[n_1,n_2]$$
$$\exp[\mathrm{i}2\pi(k_1n_1/L_{1,j} + k_2n_2/L_{2,j})]. \tag{5}$$

Curvelets are good at representing objects with curve-punctuated smoothness[16]. Palm vein images with edges are good examples of these kinds of objects. Therefore, the curvelet transform coefficients (CTCs) were used in this letter to represent the features of palm vein images. Our palm vein recognition system consists of two stages: training and classification. During training, curvelet transform was applied to decompose the images into curvelet sub-bands.

Figure 4 shows the curvelet sub-bands for a palm vein image taken from our dataset. Digital curvelet transform (scale 3, angle 16) was then applied on the original image with a size of 200×250 pixels. This produced one approximate curvelet coefficient, 16 detailed curvelet coefficients in the detail 1 layer, and 32 detailed curvelet coefficients in the detail 2 layer. It shows the approximate curvelet coefficients and 16 detailed curvelet coefficients for 16 different angles in the detail 1 layer. The images were resized to the same size for the sake of presentation.

The approximate curvelet coefficients of each palm vein image account for the maximum variance and contain maximum energy of the image-data. We selected the approximate curvelet coefficients of each image as

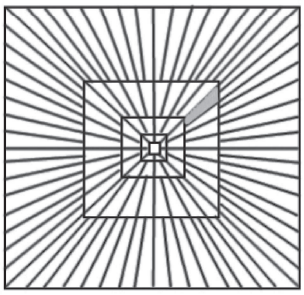

Fig. 3. Basic digital simulation of the curvelets.

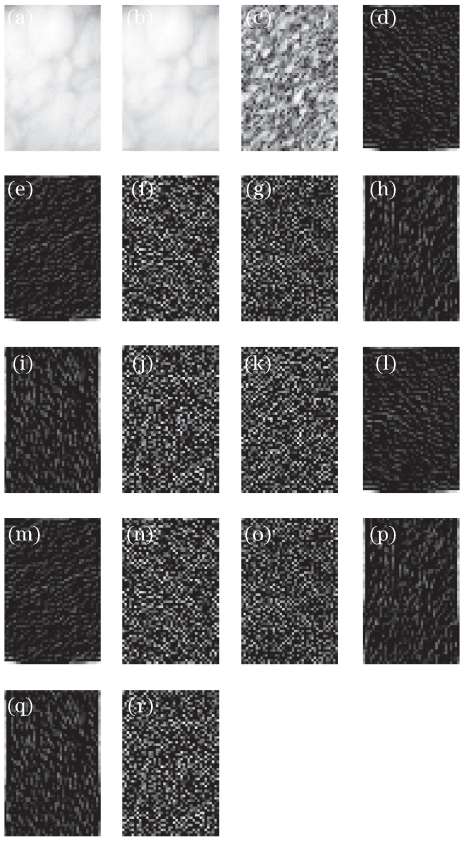

Fig. 4. Curvelet transform of the palm vein pattern. (a) The original image; (b) the approximate coefficients; (c)−(r) detailed coefficients at 16 angles in the detail 1 layer.

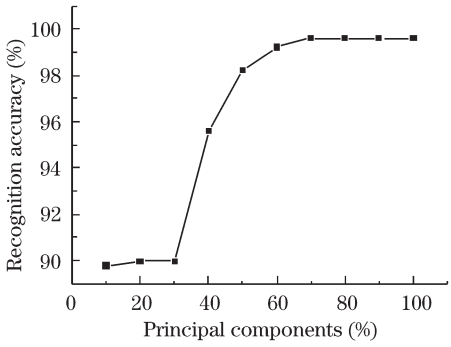

Fig. 5. Curvelet- and PCA-based results.

its first feature vector, and two other detailed sub-bands as the second and third feature vectors. Principal component analysis (PCA) was applied on the selected sub-bands for dimensionality reduction. In the classification stage, the test images were subjected to the same operations. Once the curvelet sub-images were projected to the desired feature-space, a simple NN classifier was employed with three feature vectors of each object. The classification results were obtained using the weighted Euclidean distance.

To evaluate the performance of our system, we randomly selected five images per subject from our database as the prototypes in the training stage, and used the rest for testing.

In the recognition stage, the correct recognition rate (CRR) was used to test the algorithm. The number of principal components was varied to display how the recognition rate changed with a selection of eigenvectors. Figure 5 shows that the recognition rate achieved 99.6% at principal components of 70%. The results indicate the good performance of our system.

In conclusion, a new personal recognition system using palm vein patterns is proposed. This system is convenient in acquiring vein images compared with those based on vein patterns at the back of the hand. Curvelet transform is employed to extract the features of palm vein patterns. PCA is applied on curvelet-decomposed images for dimensionality reduction. In addition, NN classifier is also used. Experimental results show that the algorithm reaches a recognition accuracy of 99.6% on the database of 500 distinct subjects. This indicates that the CTCs could represent the features of palm vein images well, and that our system has excellent recognition performance.

References

1. X. Ye, Z. He, and Z. Zhao, Chin. Opt. Lett. **6,** 487 (2008).
2. X. Fu and W. Wei, Chin. Opt. Lett. **7,** 475 (2009).
3. J. M. Cross and C. L. Smith, in *Proceedings of IEEE 29th International Carnahan Conference on Security Technology* 20 (1995).
4. S.-K. Im, H.-M. Park, S.-W. Kim, C.-K. Chung, and H.-S. Choi, *IEEE Int. Conf. Consumer Electronics Dig. Tech. Paper* 2 (2000).
5. C.-L. Lin and K.-C. Fan, IEEE Trans. Circuits and Systems for Video Technol. **14,** 199 (2004).
6. Fujitsu-Laboratories-Ltd, "Fujitsu laboratories develops technology for world's first contactless palm vein pattern biometric authentication system" http://pr.fujitsu.com/en/news/2003/03/31.html (Mar. 31, 2003).
7. L. Wang, G. Leedham, and D. S. Cho, Pattern Recognition **41,** 920 (2008).
8. S.-K. Im, H.-M. Park, Y.-W. Kim, S.-C. Han, S.-W. Kim, and C.-H. Hang, J. Korean Phys. Soc. **38,** 268 (2001).
9. Y. Wang, T. Liu, and J. Jiang, Chin. Opt. Lett. **6,** 657 (2008).
10. E. J. Candès, L. Demanet, D. L. Donoho, and L. Ying, Multiscale Modeling & Simulation **5,** 861 (2006).
11. S. Fantini and M. A. Franceschini, (eds.) *Handbook of Optical Biomedical Diagnostics* (SPIE Press, Bellingham, 2002) chap. 7.
12. L. Hong, Y. Wan, and A. Jain, IEEE Trans. Pattern Anal. Mach. Intell. **20,** 777 (1998).
13. E. J. Candès and D. L. Donoho, Comm. Pure and Appl. Math. **57,** 219 (2004).
14. E. J. Candès and D. L. Donoho, in *Curves and Surfaces*, C. Rabut, A. Cohen, and L. L. Schumaker, (eds.) (Vanderbilt University Press, Nashville, 2000) P. 105.
15. E. J. Candes and D. L. Donoho, Proc. SPIE **4119,** 1 (2000).
16. E. J. Candes, Notices of American Mathematical Society **50,** 1402 (2003).
17. P. Tao, "Robust digital watermarking in the curvelet domain", PhD. Thesis (The City University of New York, 2008).